Phys Chem Minerals (2002) 29: 65–71
DOI 10.1007/s002690100206

ORIGINAL PAPER

R. I. Mashkovtsev · V. P. Solntsev

Channel constituents in synthetic beryl: ammonium

Received: 16 May 2000 / Accepted: 5 July 2001

Abstract The infrared spectra and electron paramagnetic resonance (EPR) of channel constituents in beryls synthesized hydrothermally in the presence of NH_4Cl were investigated. Two forms of ammonium ion were observed to be incorporated into the *c*-channel. IR-spectra show the double band at 3295 and 3232 cm^{-1} and two broad bands between 2600 and 3000 cm^{-1} which were assigned to the NH_3 molecule and NH_4^+ ion, respectively. Similar N–H stretching vibrations are also observed in Regency hydrothermal synthetic beryls and can be used to separate these synthetic beryls from their natural counterparts. After γ-irradiation of hydrothermally grown samples at 77 K, the EPR of the NH_3^+(I) radical was observed. The NH_3^+(II) radical replaces the NH_3^+(I) radical when the sample is heated to room temperature. Both the NH_3 molecule and the NH_3^+ radical have their C_3 symmetry axes perpendicular to the crystal *c*-axis. The spin Hamiltonian parameters of the NH_3^+(I) are axial-symmetric due to the rapid rotation of the radical about the *c*-axis. The NH_3^+(II) radical has a low symmetry and shows a hindered rotation because of its shift from the *c*-axis position and an interaction with the proton in the near neighbourhood. Possible models for the paramagnetic centres are discussed.

Keywords Beryl · Infrared spectroscopy · EPR · Ammonium

Introduction

Beryl, with ideal formula $Al_2Be_3(Si_6O_{18})$, crystallizes in a hexagonal structure with space group $P6/mcc(D_{6h}^2)$. Its honeycomb structure consists of stacked six-membered rings $(Si_6O_{18})^{12-}$ linked together with tetrahedrally coordinated Be ions and octahedrally coordinated Al ions. The six-membered silicate rings lie one above the other along the crystal *c*-axis. This results in channels parallel to the *c*-axis (hereafter *c*-channels); these channels do not have a uniform diameter, but, instead, consist of cavities with a diameter ≈5.1 Å separated by "bottlenecks" with a diameter of about 2.8 Å. It is well known that the most common alkalis entering these channels are Na and Cs, most frequently in the presence of H_2O molecules; K and Rb may also be present in smaller amounts. The presence of H_2O and also CO_2 molecules in channels was investigated by infrared absorption more than 30 years ago (Wood and Nassau 1967). The H_2O molecules in beryl structure have been classified as type I or type II, depending on the orientation of the twofold axis of symmetry of molecule relative to the *c*-axis of beryl. Type I water molecules have their twofold symmetry axes perpendicular to the crystal *c*-axis, while the type II molecules have their symmetry axes aligned parallel to the crystal *c*-axis. The CO_2 molecules are oriented with their long axes perpendicular to the crystal *c*-axis (Wood and Nassau 1967). Normal (unsubstituted or weakly substituted) beryl shows an almost exclusive presence of type I water, whereas type II water becomes dominant when cationic substitution, in fourfold or sixfold coordination, increases (Aurisicchio et al. 1988). The presence of type II H_2O is associated with alkalis in the channels (Wood and Nassau 1967; Shatsky et al. 1981; Schmetzer 1989; Aurisicchio et al. 1988, 1994). It was concluded that H_2O molecules adjacent to alkali ions are able to rotate from perpendicular to parallel orientation by the effect of the electric field of the charged alkali cation. According to X-ray single-crystal structural refinements (Gibbs et al. 1968; Morosin 1972), type I H_2O in hydrothermally grown alkali-free synthetic beryl is located in the 2*a* position at 0,0,1/4. In high-alkali-bearing natural beryl (Hawthorne and Černý 1977; Brown and Mills 1986), water molecules and Na^+ ions are located in the 2*a* channel sites at 0,0,1/4 as well as in the smaller 2*b* channel sites at 0, 0, 0, respectively. The results of the structure analysis of a highly hydrous beryl, performed by means of pulsed

R. I. Mashkovtsev (✉) · V. P. Solntsev
United Institute of Geology, Mineralogy and Geophysics,
Novosibirsk 630090, Russia
e-mail: rim@uiggm.nsc.ru

neutron diffraction, allow an unambiguous discrimination between the Na^+ ions and the water molecules located in the channel positions 2*b* and 2*a*, respectively (Artioli et al. 1995). According to the model of Hawthorne and Černý (1977), Na^+ is bonded to either one or two neighbouring water molecules; a rough 2:1 relation between total H_2O and alkalis was indicated by Sherriff et al. (1991). However, Charoy et al. (1996) determined that in beryl from hydrothermal veins, the ratio of type II H_2O to alkalis generally exceeds two, in disagreement with data from literature obtained mainly on beryl from pegmatites.

Using electron paramagnetic resonance (EPR) for the study of the paramagnetic radicals, the H^0 spectrum was observed by Koryagyn and Grechushnikov (1966), Bershov (1970) and Samoilovich and Novozhilov (1970). The isotropic spectrum from CH_3 radicals was also observed by Bershov (1970) and Samoilovich and Novozhilov (1970). In addition, the latter authors observed EPR spectra due to H_2O^+ and OH radicals and assigned these species to channel sites, while making the unusual assignment of H^0 to a Be site. Sukharzevsky (1976) observed the formation of NO_2 radicals and assigned these radicals to interstitial sites other than channel cavities. Solntsev (1981) also observed the NO_2 and NO_3 radicals and assigned them to channel sites. Comprehensive studies of the CO_3^- molecular ions in the structural channels of beryl were conducted by Edgar and Vance (1977). Winkler (1996) demonstrated that for H_2O, static models may be inappropriate and dynamic models must be used to describe the behaviour of the H_2O molecules in beryl. It is reasonable to suggest that dynamic models could be used to describe most of the other molecules incorporated into beryl as well.

Infrared spectroscopy can be used to differentiate between natural and synthetic beryls since additional bands in the region between 3300 and 2600 cm^{-1} are observed (Leung et al. 1986). In Biron and Regency hydrothermal synthetic beryls, chlorine was invariably detected by Hänni (1982), Stockton (1984) and Kane and Liddicoat (1985). It is also known that for the growth of Regency (or Linde) hydrothermal synthetic beryls, ammonium halides are used (Nassau 1976). Based on these facts and on frequencies of the mid-range infrared features, we conclude that a system of five bands in the 3000–2600 cm^{-1} region is related to HCl molecules which predominantly form the HCl dimer in the structural channels of hydrothermal synthetic beryl (Mashkovtsev 1996). The double broad band near 3300 cm^{-1} is attributed to the NH_3 molecule that is incorporated into the structural channels of hydrothermal synthetic beryl. Recently, using the micro-proton-induced X-ray emission (micro-PIXE) technique for bulk analysis of an inclusion-free region, in some Colombian, Zambian and Brazilian beryls, chlorine was found as a structural component but in smaller amounts than in Biron hydrothermal synthetic beryls (Yu et al. 2000).

The aim of the present paper is to study ammonium in the structure of hydrothermal synthetic beryl.

Experimental

Specimens of commercially produced hydrothermal synthetic beryls (Biron, Regency and Tairus companies are the producers of synthetic beryls) as well as beryls grown in hydrothermal experiments (synthesis was performed by Dr. Pantsurkin at 1 kbar and 600 °C) in the presence of NH_4Cl were selected as a research material. Natural beryl from the Ural Mts. (Malysheva mine) was chosen for comparison. These samples were cut and polished by standard procedures with the *c*-axis lying in the plane of the plate in each case. Plate thicknesses varied from 0.15 to 1.4 mm for different samples. The mid-range infrared absorption spectra in the range of 4500–1500 cm^{-1} were recorded using a Brucker IFS 113v Fourier transform infrared spectrometer.

EPR spectra were recorded on a Radiopan SE/X 2543 spectrometer in the X-band range with a built-in NMR magnetometer. The sample was fastened on a goniometer which allowed a rotation of the crystal in the cavity around two orthogonal axes. The DPPH (diphenylpicrylhydrazyl) and MgO: Mn^{2+} references were used to calculate the g values and amounts of paramagnetic centres. The spectra were typically recorded at room temperature and at 77 K using a liquid nitrogen quartz Dewar, and the temperature control system was applied for cooling or heating the sample in the measuring cavity between 90 and 400 K.

The specimens were analyzed for Na_2O, MgO, FeO, V_2O_3, Cr_2O_3, NiO, CuO, Al_2O_3, SiO_2 and Cl using a Camebax Micro electron microprobe at an operating voltage of 15 KeV and beam current of 20 nA. The element standards were natural albite (Na_2O, Al_2O_3, SiO_2), natural orthoclase (FeO), natural diopside (MgO), natural pyrope garnet (Cr_2O_3), natural chalcopyrite (CuO), synthetic $NiFe_2O_4$ (NiO), synthetic V_2O_5 (V_2O_3 was recalculated from V_2O_5) and natural Cl-apatite. The results of microprobe analyses are listed in Table 1.

Results

Infrared spectroscopy

Figure 1 shows polarized infrared spectra for four representative samples of hydrothermal synthetic beryls and a natural beryl from the Ural Mts. Unpolarized IR spectra of experimentally grown beryl are illustrated in Fig. 2. The main spectroscopic features are listed in Table 2. The well-known bands related to water molecules are observed in the spectra from all the samples. Five absorption bands between 2600 and 3000 cm^{-1} are always seen in the Biron beryls. This system of bands

Table 1 Mean results of microprobe analyses of natural and representative synthetic beryls (wt%). *nd* = not detected

Oxides	Biron synthetic 13 points	Tairus synthetic 6 points	NH_4Cl grown synthetic 2 points	Natural Ural Mts. 2 points
SiO_2	65.66	65.8	66.1	64.45
Al_2O_3	18.16	15.95	19.1	16.75
Cr_2O_3	0.498	0.28	nd	0.1
V_2O_3	0.874	nd	nd	nd
FeO	nd	2.42	0.02	0.28
MgO	nd	0.04	nd	1.6
NiO	0.023	0.13	nd	nd
CuO	nd	0.1	0.02	nd
Na_2O	nd	0.013	nd	0.96
Cl	0.36	nd	0.026	nd

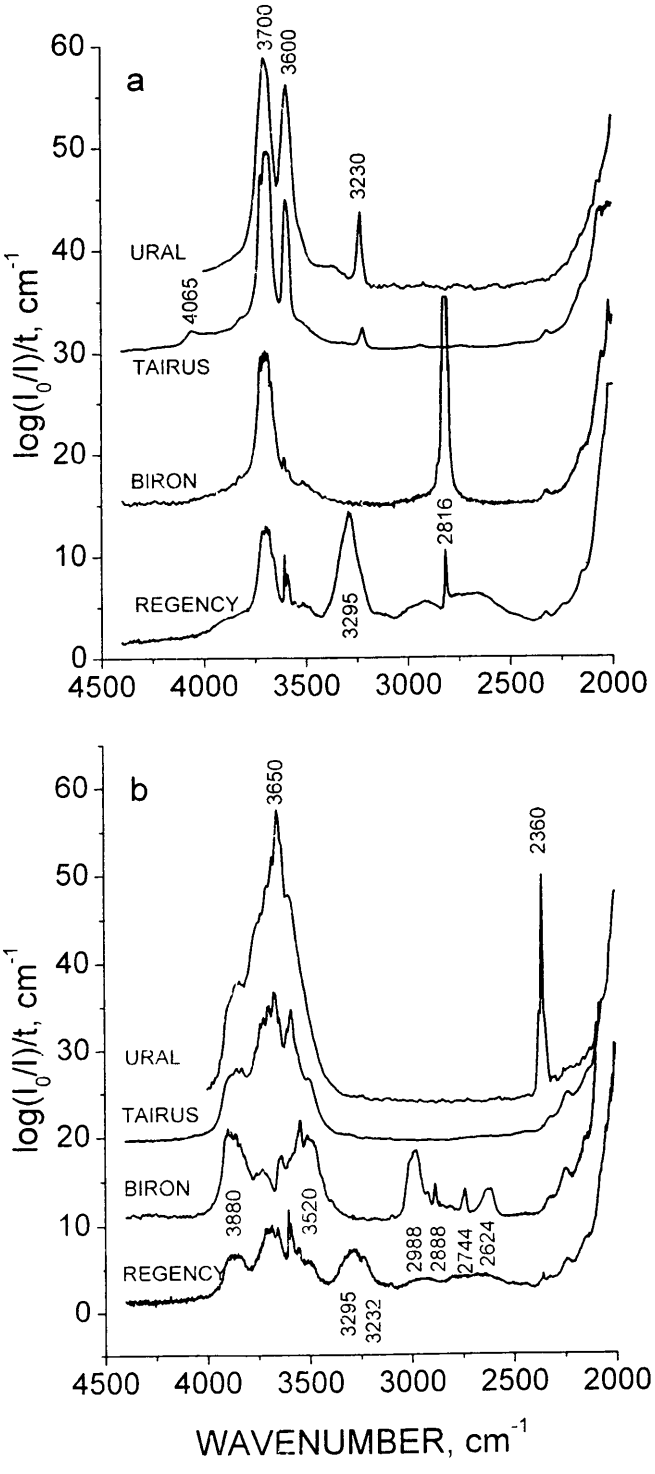

Fig. 1a, b Polarized IR spectra of thin plates of Regency, Biron and Tairus hydrothermal synthetic beryls and natural beryl from the Ural Mts. The two polarized spectra correspond to the two principal optical directions in the crystal with light polarized parallel (**a**) and perpendicular (**b**) to the optical axis. The *curves* are offset for clarity

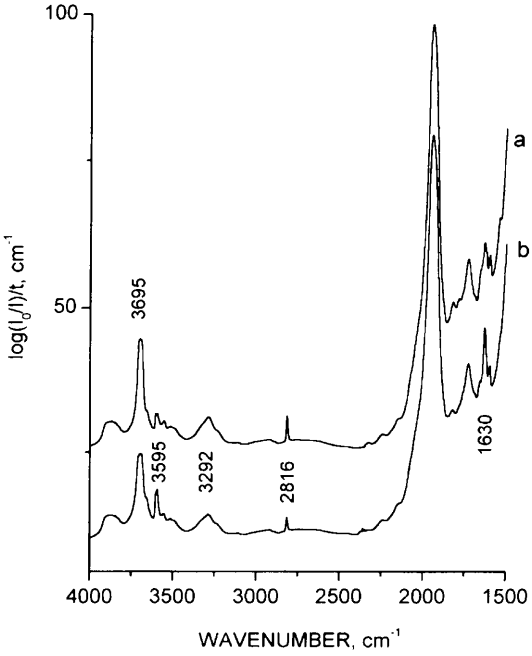

Fig. 2a, b Unpolarized IR spectra of thin plate of beryl hydrothermally grown in the presence of NH_4Cl. Uneven distribution of channel constituents is illustrated by two spectra taken in different points, **a** and **b**, of the same plate

may be so weak in the Regency beryl that only the central band at 2816 cm^{-1} was observed on the background of the other broad bands. The system consists of a main band at 2816 cm^{-1} and two pairs of bands (one at 2624 and 2988 cm^{-1} and another at 2744 and 2888 cm^{-1}) which are located almost symmetrically about the main band, whereas the intensities of the bands at 2624 and at 2744 cm^{-1} are always weaker than those of their counterparts at 2888 and at 2988 cm^{-1}. In a solid Ar matrix, the spectrum of the T-shaped HCl dimer has one very weak band at 2855 cm^{-1} and another strong band at 2817.5 cm^{-1}, which depends only slightly on the matrix (Hallam 1973; Mailard et al. 1979). Therefore, we assume that the strong band at 2816 cm^{-1}, observed in the IR spectra of beryl, is related to the stretching vibration of the H–Cl bond of one HCl molecule which is hydrogen-bonded with the chlorine atom of the second HCl molecule, and the two-pair bands around can be assigned to librations of the two molecular axes about their equilibrium configurations.

An additional poorly resolved doublet at 3295 and 3232 cm^{-1} was observed in the Regency beryls. Spectra like those in the Regency beryls were observed in experimental beryls grown in an NH_4Cl salt solution medium (see Fig. 2). We assign the two broad bands between 2600 and 3000 cm^{-1} to the absorption of the NH_4^+ ion (cf. Ryskin 1974; Krasnov 1979). We have tentatively attributed the doublet at 3295 and 3232 cm^{-1} to the vibrational stretching of the N–H bonds in the NH_3 molecule (cf. El'yashevich 1962; Krasnov 1979). Referring to El'yashevich (1962), we interpret the characteristic NH_3 spectrum in beryl as follows. In the 3-μm region there must be two bands corresponding to the symmetric stretching vibration ν_1 and asymmetric stretching vibration ν_3 for the free NH_3 molecule. Their polarizations correspond to those in Table 2, provided

Table 2 The main features of the mid-infrared spectra of hydrothermal synthetic and Ural beryls and their appearance in beryls of different origin[a]

Peak location, cm^{-1}	Polarization relative to *c*-axis	Beryl type				Assignment[b]
		Biron	Regency	Tairus	Ural	
2360	⊥				s	ν_3 CO_2 [a]
2624	⊥	m	w – uo			$\nu_d - \nu_{lib}$ $(HCl)_2$ [b]
2600–2700	∥, ⊥		w			$\nu_2 + \nu_4$, $2\nu_4$ NH_4^+ [c]
2744	⊥	m	w – uo			$\nu_d - \nu'_{lib}$ $(HCl)_2$ [c]
2816	∥	vs	s – w			ν_d $(HCl)_2$ [b]
2888	⊥	m	w – uo			$\nu_d + \nu'_{lib}$ $(HCl)_2$ [c]
~2940	∥, ⊥		w			ν_3 NH_4^+ [c]
2988	⊥	s	m – uo			$\nu_d + \nu_{lib}$ $(HCl)_2$ [b]
3230	∥			m – w	s – m	$2\nu_2$ H_2O II [a]
3232	⊥		sh			ν_1 NH_3 [b]
3295	∥, ⊥		s – m			ν_3 NH_3 [b]
3520	⊥	w	w	w	m	H_2O I [a]
3560	⊥			w	w	ν_1 H_2O I [a]
3596	∥	vw	vw	m	s	ν_1 H_2O II [a]
3608	∥	w	w	w		OH [d]
3655	⊥			w	m	ν_3 H_2O II [a]
3695	∥	s	s	s	vs	ν_3 H_2O I [a]
3880	⊥	m	m	m	s	$\nu_1 + \nu_{lib}$ H_2O I [a]

[a] m – moderate, s – strong, w – weak, vw – very weak, vs – very strong, uo – unobserved, sh – shoulder; ν_{lib} – libration mode, ν_d – frequency of the main peak of HCl dimer
[b] References: [a] Wood and Nassau (1967); [b] Mashkovtsev (1996); [c] this work; [d] Mashkovtsev and Lebedev (1992)

that the threefold axis of symmetry of the NH_3 molecule is directed perpendicularly to the *c*-axis of beryl.

Figure 2 shows an uneven distribution of ammonium through the plate of experimental beryl. From a comparison of curves (a) and (b) in Fig. 2, it is seen that the intensity of the bands at 3600 and 1630 cm^{-1} related to type II H_2O increases, whereas there is a decrease in absorptions related to the NH_4^+ ion, NH_3 molecule and type I H_2O. The amounts of ammonium and water molecules are comparable if water molecules are assumed to substitute for ammonium in the structural channels. The solution from which synthetic beryl was grown did not contain any alkalis (Dr. Pantsurkin, personal communication), and sodium ions were not detected in the NH_4Cl-grown samples studied (see Table 1). Hence, the type II H_2O is not necessarily located close to an alkali ion.

Electron paramagnetic resonance

Additional investigation on the experimentally grown beryls was needed for a further understanding of ammonium incorporation into the beryl structure.

In the original crystals Cr^{3+} is the only paramagnetic centre. The samples were irradiated with γ-rays (Co^{60}, dose 5 Mrad) at 77 K and at ambient temperature to induce additional paramagnetic centres.

Figure 3 shows the EPR spectrum obtained from γ-irradiated beryl at 77 K and then measured at 77 K. This spectrum consists of the known doublet related to the hydrogen atom H^0 (Koryagyn and Grechushnikov 1966) and of an additional pattern of lines. This pattern consists of three quartets with an intensity ratio 1:3:3:1,

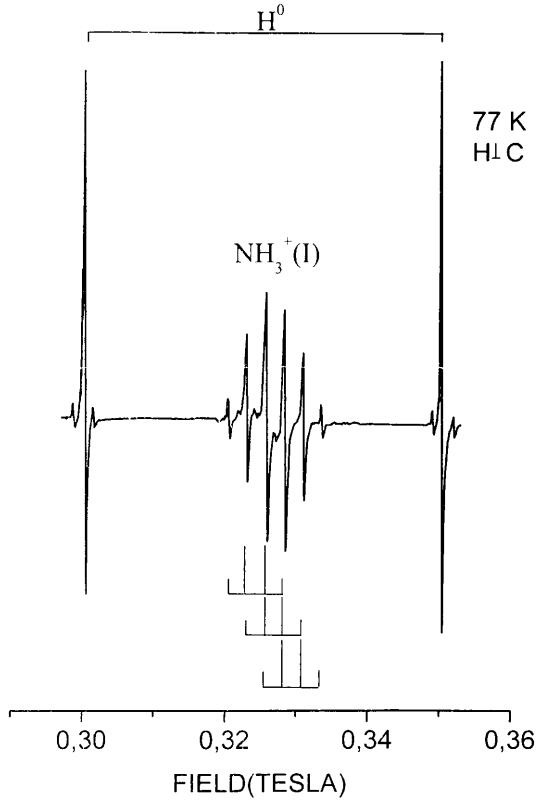

Fig. 3 EPR spectrum of γ-irradiated at 77 K synthetic ammonium-doped beryl with the magnetic field perpendicular to the *c*-axis. Three quartets are marked by the *stick diagram*. The HFI with nitrogen and protons of the NH_3^+(I) radical are equal in magnitude in this direction

Table 3 Spin Hamiltonian parameters for NH_3^+ radicals in beryl. The angle θ is the deviation from crystal *c*-axis

Radical T K	g-tensor ±0.0005	A-tensor (±1 MHz)		
		H	N	θ
NH_3^+(I) 77	$g_{\|\|}$ 2.0035	$A_{\|\|}$ 65	14.9	0
	$g_\perp$ 2.0037	$A_\perp$ 73.5	73.5	90
NH_3^+(II) 300	g_1 2.0039	A_1 63.1	19.6	23
	g_2 2.0034	A_2 65.9	57.2	113
	g_3 2.0030	A_3 65.9	79.9	90

which is expected to originate from hyperfine interactions (HFI) with one nucleus of spin 1 (^{14}N, 100% natural abundance) and three nuclei of spin 1/2 (^1H, 100% natural abundance), and certainly arises from the rotating NH_3^+ radical (Cole 1961; Fujimoto and Morton 1965; Yu et al. 1988; Rao and Sunandana 1995). As a result of its rotation, this paramagnetic radical [labelled NH_3^+(I)] has a uniaxial symmetry about the *c*-axis in the crystal structure. A drastic decrease in the intensity of the NH_3^+(I) and H^0 centres was observed, because of their annealing, after allowing the sample to warm up to room temperature followed by measurement at 77 K. A new centre, NH_3^+(II), appeared, while the NH_3^+(I) centre decreased. At 77 K, the spectra of the residual NH_3^+(I) and NH_3^+(II) centres were observed together, but at 300 K only the spectrum of the NH_3^+(II) centre was observed. The signal for the NH_3^+(I) radical was not detected at temperatures higher than 90 K. The principal values and axes for the spin Hamiltonian tensors of the NH_3^+ radicals in beryl are listed in Table 3. The *a* and *b* crystallographic axes cannot be identified by single-crystal X-ray difraction because of the hexagonal symmetry of beryl. As a consequence, the angular dependence of the spectra was measured in the radical system of coordinates, and the principal axes of the spin Hamiltonian tensors were characterized only by the angle θ made with the *c*-axis. One and six magnetically inequivalent positions in the unit cell were observed for the NH_3^+(I) and NH_3^+(II) centres, respectively. The spectrum of NH_3^+(I) is independent of the rotation around the *c*-axis and the three spectra of NH_3^+(II) alternate in 60° intervals.

Figure 4 shows the EPR spectra of the NH_3^+(II) centre at room temperature. As may be seen in Fig. 4b, all the lines for the NH_3^+(II) spectrum are split into doublets. This is certainly due to a proton located in the neighbourhood of the radical. The magnitude of this superhyperfine splitting varies from nearly zero to a maximum of 6.7 MHz in the direction near to that of the HFI minimum for nitrogen A_1. The superhyperfine structure is poorly resolved because of broad resonance lines for arbitrary orientations of the crystal in the magnetic field.

At 77 K, the spectrum for the NH_3^+(II) radical is more difficult to interpret, as the radical is no longer rapidly rotating in the beryl structure. Furthermore,

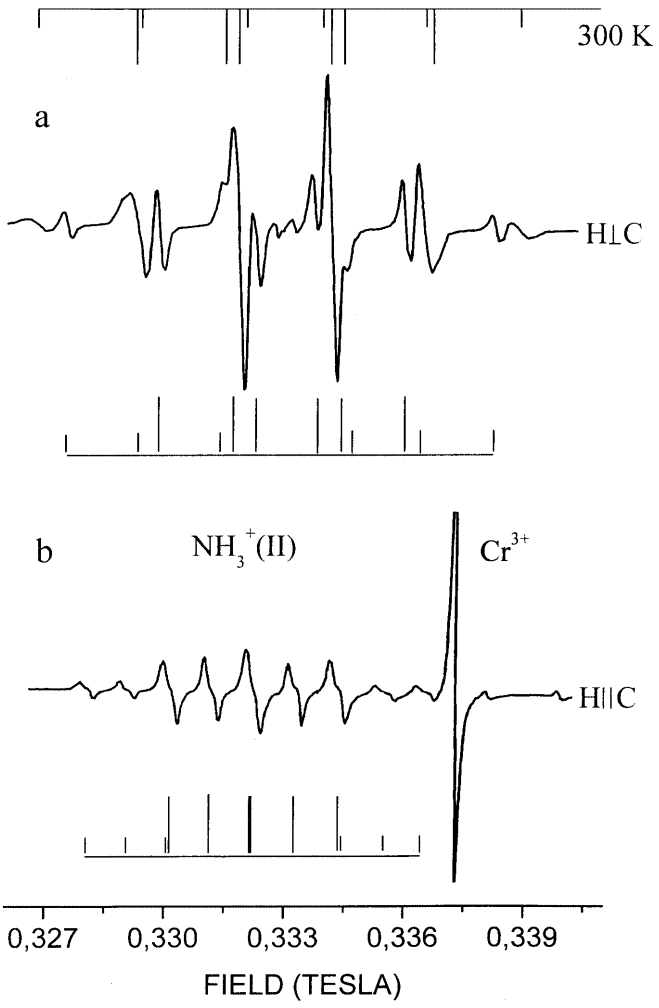

Fig. 4 EPR spectra of synthetic ammonium-doped beryl γ-irradiated at 300 K. There is an additional doubling of lines of the NH_3^+(II) radical in the spectrum recorded with the magnetic field applied parallel to the *c*-axis

broad lines of the NH_3^+(II) spectrum are superimposed on the residual signal from the NH_3^+(I) radical. Because of this, at 77 K we measured only the maximum equal to the 123 MHz of the nitrogen HFI when the magnetic field was applied perpendicular to the *c*-axis.

The NH_3^+ radicals were annealed at near 150 °C and may again be induced by the same irradiation. The NH_3^+(II) and the trace of the NH_3^+(I) radicals were also observed after irradiation at ambient temperatures.

Discussion

As can be seen from the IR spectra, both the natural and the Tairus beryls have no absorption bands at 3295 cm^{-1} or in the range between 2600 and 3000 cm^{-1}. Synthesis of the Tairus and Regency (Nassau 1976) hydrothermal beryls involves HF and ammonium halide solutions, respectively. Hence, we assume from the IR spectra that ammonium (as NH_4^+) was incorporated

only in beryls grown using the NH_4Cl in solution. Under γ-irradiation, the NH_3^+ radical may be generated both from NH_3 and NH_4^+. Although part of the NH_3 (or NH_4^+) was transformed to the NH_3^+ radical, the intensity of the bands related to NH_3 and NH_4^+ in the IR spectra showed no detectable decrease after γ-irradiation. The concentrations of the NH_3^+ radical measured from EPR (290 ppm) were too small to result in some change in the IR spectra.

The equilibrium structure of the NH_3^+ radical is known to be planar, having the unpaired $2p\pi$ orbital of the nitrogen atom along the threefold symmetry axis. A model predicts that the anisotropy of the nitrogen HFI has its maximum along the threefold axis (Cole 1961). In NH_4ClO_4 the ammonium radical was found to be tumbling rather freely in the structure at room temperature (Cole 1961; Fujimoto and Morton 1965). This tumbling almost averages out the anisotropy of the nitrogen HFI (Table 4); but at 77 K, the HFI tensor has a nearly uniaxial symmetry, and the result was interpreted as due to a rotational motion of the NH_3^+ radical. At 4 K the ammonium radical is no longer rapidly rotating in the crystal (Fujimoto and Morton 1965). The values of HFI for nitrogen in beryl, as shown in Table 4, are smaller (i.e. 124.8 MHz at 4 K) than those expected from a rigidly oriented radical NH_3^+ in NH_4ClO_4 (Fujimoto and Morton 1965). This implies the presence of a motion of the NH_3^+ radical in the structure of beryl. Free rotation of the threefold axis of the NH_3^+(I) radical at 77 K around the *c*-axis averages out the A_2 and A_3 HFI. In contrast, even at 300 K, the NH_3^+(II) is undergoing restricted rotation about a principal direction which is tilted at 23° to the *c*-axis, probably due to the interaction with an additional proton. This rotation partially averages out the anisotropy of the nitrogen HFI. The restricted freedom of the NH_3^+(II) radical to rotate is frozen out near 77 K (the most HFI for the nitrogen is 123 MHz at 77 K). As one can see from Table 3, the average values of HFI with proton and nitrogen for NH_3^+(II) are smaller than for the NH_3^+(I) radical because of a weak transfer of electron density to the additional proton.

The NH_4^+ has ionic radius of 1.61 Å, between that of Rb^+ (1.52 Å) and Cs^+ (1.67 Å), the NH_3 has a dimension (the N–H distance is about 1.07 Å) comparable to Na^+ ion (1.02 Å) (Shannon 1976), hence they may enter into the *c*-channel of the beryl structure. There are two crystallographically distinct sites at 0,0,1/4 (site 2*a*) and at 0,0,0 (site 2*b* at the centre of the six-membered rings) in the *c*-channels, which, in high-alkali-bearing natural beryl, are occupied by water molecules and Na^+ ions, respectively (Hawthorne and Černý 1977; Brown and Mills 1986). The ammonium radical can be located at both sites. The EPR of the NH_3^+(I) radical was not observed at temperatures slightly above 77 K due to line broadening. A possible reason for this broadening is that NH_3^+(I) gains the additional freedom to tumble and to move at elevated temperatures. The conversion of the NH_3^+(I) radical to NH_3^+(II) may be explained in the following way. After γ-irradiation the ammonium radical can hold still for very long at 77 K. However, most of the NH_3^+(I) are positively charged ion-radicals and, on heating, can move to some sites that bear excessive negative charge. Then it is possible that the double superhyperfine splitting observed for NH_3^+(II) is due to the OH^- ion. Under the influence of γ-irradiation the H^0 and OH radicals have to form as a result of H_2O radiolysis: $H_2O \rightarrow H + OH$ (Koryagyn and Grechushnikov 1966). However, no paramagnetic OH radical was observed by EPR after γ-irradiation of our beryls. The OH radical transforms to OH^- ion most likely by electron capture. The presence of the OH^- ions, either in the oxygen sites or in the structural channels of beryl, has also been suggested by other authors (Schmetzer 1989; Sherriff et al. 1991; Aurisicchio et al. 1994). We cannot locate both the NH_3^+(II) radical and OH^- ion in any adjacent structural positions in the *c*-channel, as in this case the NH_3^+(II) would be oriented with its principal direction along the *c*-axis. Alternatively, we can assign the NH_3^+(II) radical to the cavity of the structural channel and the OH^- group to the oxygen position O1 that belongs to the six-membered ring. In the next-nearest neighbourhood a deficiency of Be^{2+} is possible (in our beryl some vacancies are needed for charge balance of positive ions in the channels). The OH^- group can also be formed by the H^0 radical that is annealed simultaneously with the NH_3^+(I) radical at room tem-

Table 4 Comparison of the nitrogen hyperfine tensor (MHz) in beryl and NH_4ClO_4 (Fujimoto and Morton 1965)

Radical	T K	A_1	A_2	A_3	A_{iso}
NH_3^+(I)	77	14.9	73.5	73.5	54
NH_3^+(II)	300	19.6	57.2	79.9	52.2
NH_3^+:	4	10.7	29.2	124.8	54.9
(NH_4ClO_4)	77	27.9	34.2	100.5	54.2
	300	49.6	52.2	61.1	54.2

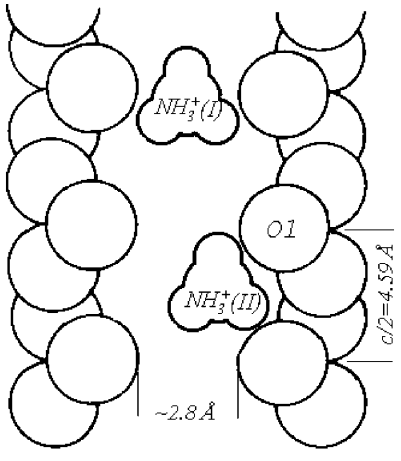

Fig. 5 The proposed model for the NH_3^+ paramagnetic centres in structural *c*-channel of beryl. The NH_3^+(II) radical is displaced from *c*-axis position in one of the six equivalent directions

perature, in contrast to natural beryl in which the atomic hydrogen is annealed at 600 K (Samoilovich and Novozhilov 1970). The angle between the 2*a*-O1 vector and *c*-axis is 48°, which differs markedly from the angle of 23° between the principal direction of the ammonium radical and the *c*-axis. Then the NH_3^+(II) must be displaced from the *c*-axis position in one of the six equivalent directions towards the wall of the *c*-channel to fit the principal direction of ammonium radical and the six magnetically inequivalent species observed experimentally. A possible model for the NH_3^+ paramagnetic centres is demonstrated in Fig. 5.

Acknowledgements The authors thank the following for lending material for this study: Dr. A. S. Lebedev and S. D. Pantsurkin (Institute of Mineralogy and Petrography, Novosibirsk), Dr. O. V. Kholdeev (Tairus joint venture, Novosibirsk). We wish to thank Dr. S. Z. Smirnov for microprobe analyses. Helpful comments on an earlier version of the manuscript by two anonymous reviewers are much appreciated.

References

Artioli G, Rinaldi R, Wilson CC, Zanazzi PF (1995) Single-crystal pulsed neutron diffraction of a highly hydrous beryl. Acta Crystallogr (B) 51: 733–737

Aurisicchio C, Fioravanti G, Grubessi O, Zanazzi PF (1988) Reappraisal of the crystal chemistry of beryl. Am Mineral 73: 826–837

Aurisicchio C, Grubessi O, Zecchini P (1994) Infrared spectroscopy and crystal chemistry of the beryl group. Can Mineral 32: 55–68

Bershov LV (1970) Methane and atomic hydrogen in some natural minerals. Geochemistry 7: 853–856

Brown GE, Mills BA (1986) High-temperature structure and crystal chemistry of hydrous alkali-rich beryl from the Harding pegmatite, Taos Country, New Mexico. Am Mineral 71: 547–556

Charoy B, de Donato P, Barres O, Pinto-Coelho C (1996) Channel occupancy in alkali-poor beryl from Serra Branca (Goias, Brazil): spectroscopic characterization. Am Mineral 81: 395–403

Cole T (1961) Paramagnetic defects in irradiated NH_4ClO_4. J Chem Phys 35: 1169–1173

Edgar A, Vance ER (1977) Electron paramagnetic resonance, optical absorption and magnetic circular dichroism studies of the CO_3^- molecular-ion in irradiated natural beryl. Phys Chem Miner 1: 165–168

El'yashevich MA (1962) Atomic and molecular spectroscopy. Fizmatgiz, Moscow, USSR, 892 p

Fujimoto M, Morton JR (1965) Electron spin resonance spectra of ^{15}N-centered radicals at low temperatures. I. The radical NH_3^+ trapped in NH_4ClO_4. Can J Chem 43: 1012–1016

Gibbs GV, Breck DV, Meagher ED (1968) Structural refinement of hydrous and anhydrous synthetic beryl, $Al_2(Be_3Si_6)O_{18}$ and emerald, $Al_{1.9}Cr_{0.1}(Be_3Si_6)O_{18}$. Lithos 1: 275–285

Hallam HE (1973) Molecules trapped in low-temperature matrices. In: Hallam HE (ed) Vibrational spectroscopy of trapped species: infrared and Raman studies of matrix-isolated molecules, radicals and ions. Wiley-Interscience, New York, pp 68–132

Hänni HA (1982) A contribution to the separability of natural and synthetic emeralds. J Gemmol 18: 138–144

Hawthornef C, Černý P (1977) The alkali-metal positions in Cs-Li beryl. Can Mineral 15: 414–421

Kane E, Liddicoat RT (1985) The Biron hydrothermal synthetic emerald. Gems Gemol 21: 156–170

Koryagyn VF, Grechushnikov BN (1966) EPR of atomic hydrogen in beryl. Sov Phys: Sol State 7: 2010–2012

Krasnov KS (1979) Molecular constants of inorganic compounds. Handbook, Khimiya, Leningrad, USSR, 448 p

Leung CS, Merigoux H, Poirot JP, Zecchini P (1986) Use of infrared spectrometry in gemmology. In: Proceedings of the 13th General Meeting of the International Mineralogical Association, 1982, Varna, vol. 2. Sofia, pp 441–448

Mailard D, Schriver A, Perchard JP (1979) Study of hydracids trapped in monoatomic matrices. I. Near-infrared spectra and aggregate structures. J Chem Phys 71: 505–516

Mashkovtsev RI (1996) The application of spectroscopy to discern natural and synthetic emeralds. In: Annual Meeting of the Russian Mineralogical Society, 1996, Saint Petersburg, pp 47–48

Mashkovtsev RI, Lebedev AS (1992) Infrared spectroscopy of water in beryl. J Struct Chem 33: 930–933

Morosin B (1972) Structure and thermal expansion of beryl. Acta Crystallogr (B)28: 1899–1903

Nassau K (1976) Synthetic emerald: the confusing history and the current technologies. J Crystal Growth 35: 211–222

Rao YS, Sunandana CS (1995) NH_3^+ EPR in single crystal potassium ammonium sulphate, KNH_4SO_4. Sol State Commun 94: 563–567

Ryskin YI (1974) The vibrations of protons in minerals: hydroxyl, water and ammonium. In: Farmer VC (ed) The infrared spectra of minerals. Mineral Soc London, pp 137–182

Samoilovich MI, Novozhilov AI (1970) EPR spectrum of the (H_3C), $(H_2O)^+$, (OH) radicals and atomic hydrogen in beryl. Zh Neorg Khim 15: 84–86

Schmetzer K (1989) Types of water in natural and synthetic emerald. N Jb Miner Mh 1: 15–26

Shannon RD (1976) Revised effective ionic radii and systematic studies of interatomic distances in halides and halcogenides. Acta Crystallogr (A) 32: 751–767

Shatsky VS, Lebedev AS, Pavlyuchenko VS, Kovaleva LT, Kozmenko OA, Yudin AN, Belov NV (1981) Study of conditions of entering of alkaline cations in the beryl structure. Geokhimiya 3: 351–360

Sherriff BL, Grundy HD, Hartman JS, Hawthorne FC, Černý P (1991) The incorporation of alkalis in beryl: multi-nuclear MAS NMR and crystal-structure study. Can Mineral 29: 271–285

Solntsev VP (1981) Nature of color centres and EPR in beryl and chrysoberyl. In: Trudy Instituta Geologii i Geofiziki, Akademia Nauk SSSR, issue 499. Novosibirsk, pp 92–140

Stockton CM (1984) The chemical distinction of natural from synthetic emeralds. Gems Gemol 20: 141–145

Sukharzhevsky SM (1976) Study of the NO_2 molecular structure in beryl. In: Voprosy geokhimii i typomorphysm mineralov, issue 1. Leningrad, pp 22–29

Winkler B (1996) The dynamics of H_2O in minerals. Phys Chem Miner 23: 310–318

Wood DL, Nassau K (1967) Infrared spectra of foreign molecules in beryl. J Chem Phys 47: 2220–2228

Yu JT, Chou SY, Huang SJ (1988) Low-temperature phase transitions of $LiCsSO_4$: ESR of NH_3^+ and Cr^{5+}. J Phys Chem Sol 49: 289–297

Yu KN, Tang SM, Tay TS (2000) PIXE studies of emeralds. X-Ray Spectrom 29: 267–278